



## Direct Measurement of the $W$ Boson Width in $p\bar{p}$ Collisions at $\sqrt{s} = 1.96$ TeV

The DØ Collaboration  
(Dated: August 23, 2004)

This note describes a direct measurement of the  $W$  boson total decay width  $\Gamma_W$  using the DØ detector at the Fermilab Tevatron Collider. The measurement uses an integrated luminosity of  $177.3 \text{ pb}^{-1}$ , collected during the 2002-2003 run. The width is determined by normalizing the predicted signal and background transverse mass distributions to 75,285  $W \rightarrow e\nu$  candidates in the transverse mass region  $50 < M_T < 100$  GeV and then fitting the predicted shape to the 625 candidates in the tail region  $100 < M_T < 200$  GeV. The  $W$  width is determined to be  $\Gamma_W = 2.011 \pm 0.093$  (stat)  $\pm 0.107$  (syst) GeV.

*Preliminary Results for Summer 2004 Conferences*

## I. INTRODUCTION

The  $W$  boson width  $\Gamma_W$  is precisely predicted to be  $\Gamma_W = 2.090 \pm 0.008$  GeV in terms of the masses and coupling constants of the gauge bosons [1]. It has been measured indirectly to be  $2.141 \pm 0.057$  GeV [2] using the  $W/Z$  cross section ratio  $R = \frac{\sigma(p\bar{p} \rightarrow W+X) \times Br(W \rightarrow l\nu)}{\sigma(p\bar{p} \rightarrow Z+X) \times Br(Z \rightarrow ll)} = \frac{\sigma(W)}{\sigma(Z)} \frac{\Gamma(Z)}{\Gamma(Z \rightarrow ll)} \frac{\Gamma(W \rightarrow l\nu)}{\Gamma_W}$ , by assuming SM values for  $\sigma(W)/\sigma(Z)$  and  $\Gamma(W \rightarrow l\nu)$  and using the LEP measurements of the leptonic branching ratio  $Br(Z \rightarrow ll) = \frac{\Gamma(Z \rightarrow ll)}{\Gamma(Z)}$ . Recently CDF reported a new indirect measurement at  $\sqrt{s} = 1.96$  TeV and the result is  $2.079 \pm 0.041$  GeV [3]. Direct measurement of the  $W$  boson width have been obtained from the transverse mass spectrum of  $W \rightarrow l\nu$  decays by the CDF and DØ experiments using data collected during Run I of the Tevatron. The results are  $\Gamma_W = 2.05 \pm 0.13$  GeV (CDF) [4] (using  $W \rightarrow e\nu$  and  $W \rightarrow \mu\nu$  decays) and  $\Gamma_W = 2.231_{-0.170}^{+0.175}$  GeV (DØ) [5] (only  $W \rightarrow e\nu$  decays). These results have been combined, considering correlations in the systematic uncertainties, to obtain  $\Gamma_W = 2.115 \pm 0.105$  GeV [2]. Direct measurements of  $\Gamma_W$  have also been made by measuring the  $W$  resonance lineshape in  $e^+e^- \rightarrow W^+W^-$  events collected at the LEP  $e^+e^-$  collider, resulting in an average value  $\Gamma_W = 2.150 \pm 0.091$  GeV [6].

This note presents a direct measurement of  $\Gamma_W$  obtained in studies of the transverse mass spectrum of  $W \rightarrow e\nu$  events. The  $W$  boson transverse mass is defined as  $M_T = \sqrt{2E_T^e E_T^\nu (1 - \cos(\phi_e - \phi_\nu))}$ , where  $E_T^e$ ,  $E_T^\nu$  are the transverse energies and  $\phi_e$ ,  $\phi_\nu$  are azimuthal angles of electron and neutrino respectively. The transverse mass distribution exhibits a Jacobian edge near  $M_W$ , events with  $M_T > M_W$  arise from a combination of the non-zero  $W$  width and detector resolutions. Figure 1 shows the Monte Carlo simulated  $M_T$  spectra for different  $W$  boson widths. At low values of  $M_T$  these distributions show little sensitivity to the value of  $\Gamma_W$ ; differences show up only in the tail region, where the Breit-Wigner lineshape (width component) dominates over the Gaussian lineshape (detector resolution component).

Since there is no analytic description of the transverse mass distribution as observed in data, the determination of  $M_T$  relies on modelling the transverse mass spectrum through a Monte Carlo simulation. The Monte Carlo simulation depends on experimental data for its parameters.  $Z \rightarrow ee$  data are extensively used for the calibration of the simulation process.

In this analysis the  $W$  width is determined from a binned maximum likelihood fit to the transverse mass distribution in the region  $100 < M_T < 200$  GeV. The choice  $M_T > 100$  GeV minimizes the total error.

## II. DØ DETECTOR

The DØ detector is comprised of the following main elements [7]. Charged particle momenta are measured using a magnetic central-tracking system, which consists of a silicon microstrip tracker (SMT) and a central fiber tracker (CFT), both located within a 2 T superconducting solenoidal magnet [8]. Central and forward preshower detectors are located just outside of the superconducting coil (in front of the calorimetry). They are constructed from several layers of extruded triangular scintillator strips that are read out using wavelength-shifting fibers and VLPCs, and are used for electron and photon identification. The next layer of detection involves three liquid-argon/uranium calorimeters: a central section (CC) covering  $|\eta|$  up to  $\approx 1$ , and two end calorimeters (EC) extending coverage to  $|\eta| \approx 4$ , all housed in separate cryostats [9]. In addition to the preshower detectors, scintillators between the CC and EC cryostats provide sampling of developing showers at  $1.1 < |\eta| < 1.4$ .

A muon system resides beyond the calorimetry, and consists of tracking detectors and scintillation trigger counters before the 1.8 T toroids, followed by two more similar layers after the toroids. Tracking at  $|\eta| < 1$  relies on 10 cm wide drift tubes [9], while 1 cm mini-drift tubes are used at  $1 < |\eta| < 2$ .

The luminosity is measured using plastic scintillator arrays located in front of the EC cryostats, covering  $2.7 < |\eta| < 4.4$ . The trigger and data acquisition systems are designed to accommodate the large instantaneous luminosity of Run II.

## III. DATA SAMPLE AND EVENT SELECTION

The data sample used here was collected with the DØ detector during the 2002-2003 run using a single electron trigger based solely on calorimetric information. Bad quality data are removed from the sample, leaving a total of  $177.3 \text{ pb}^{-1}$  of integrated luminosity.

Electrons and photons are first identified as electromagnetic (EM) clusters found in the central calorimeter using a simple cone algorithm. The fraction of energy in the EM calorimeter within the cone,  $f_{EM}$ , is required to be greater than 0.9. Shower shape and isolation requirements distinguish the EM objects from hadronic jets.

The missing transverse momentum is calculated by taking the vector sum  $\vec{E}_T = -\sum_i E_i \sin\theta_i \hat{u}_i$ , where the sum runs over all calorimeter cells that were read out except cells in the coarse hadronic section,  $E_i$  is the energy deposited in the  $i$ th calorimeter cell,  $\theta_i$ ,  $\hat{u}_i$  are the angle and the direction defined by the cell center and the event vertex.

For this analysis, we require a candidate electron in the fiducial region of the central calorimeter with  $|\eta^{det}| < 1.05$ ,  $f_{EM} > 0.9$ ,  $f_{iso} < 0.15$ ,  $\chi^2(HM7) < 12$  and transverse energy  $E_T > 25$  GeV. The isolation fraction  $f_{iso}$  measures the ratio between the energy measured in the ring between  $\Delta R = 0.2$  and  $0.4$  around the electron direction and the energy in the  $\Delta R = 0.2$  cone. The  $\chi^2(HM7)$  variable measures the consistency of the shower shape with that expected for an electromagnetic shower. The electron candidate is also required to have a track that coincides spatially and to have an  $E/p$  ratio consistent with that of an electron.

The  $Z \rightarrow ee$  candidate events used for tuning the simulation must have at least 2 candidate electrons, one of which must have fired one of the single electron triggers. Both electron candidates are required to pass the same selection criteria used for the selection of the  $W \rightarrow e\nu$  candidates. This resulted in a sample of 3,169 candidate events with an invariant mass between 0 and 150 GeV.

The  $W \rightarrow e\nu$  candidate events must have at least 1 electron candidate with a matched track, matching the trigger requirements for the event. In addition we require the events to have a missing transverse energy  $E_T > 25$  GeV and the W boson to have a transverse momentum  $p_T^W < 20$  GeV. To remove the background from non identified  $Z \rightarrow ee$  decays, we also veto events with a second isolated track event with  $p_T > 15$  GeV recoiling against the candidate electron. This selection resulted in a sample of 75,910 candidate events with transverse mass between 50 to 200 GeV, and 625 candidate events with transverse mass between 100 to 200 GeV.

#### IV. MONTE CARLO SIMULATION

We use a parameterized model to simulate the detector response and resolution and thus obtain the prediction for the observed electron and recoil momenta.

To simulate the detector response to an electron of energy  $E_0$ , we compute the observed energy as

$$E(e) = R_{EM}(E_0) \otimes \sigma_{EM}(E_0) \quad (1)$$

where  $R_{EM}(E_0)$  is the response of the electromagnetic calorimeter and  $\sigma_{EM}$  is the energy resolution of the electromagnetic calorimeter. The energy response  $R_{EM}(E_0)$  is modelled using two parameters  $\alpha$  and  $\beta$ :  $R_{EM}(E_0) = \alpha \times E_0 + \beta$ , where  $\alpha$  is the EM energy scale and  $\beta$  EM energy offset. The resolution  $\sigma_{EM}(E_0)$  is also modelled using two parameters  $C_{EM}$  and  $S_{EM}$ :  $\sigma_{EM}(E_0)/E_0 = \sqrt{C_{EM}^2 + S_{EM}^2/E_0}$ , where  $C_{EM}$  is the constant term and  $S_{EM}$  the sampling term for the EM calorimeter.

The calorimeter position resolution is modelled using two parameters  $\sigma_\eta$  and  $\sigma_\phi$ :  $\eta_{smear} = \eta_{gen} + x * \sigma_\eta$  and  $\phi_{smear} = \phi_{gen} + y * \sigma_\phi$ , where  $\sigma_\eta$  and  $\sigma_\phi$  are  $\eta$  and  $\phi$  resolutions,  $x$  and  $y$  are random variables from a normal distribution.

The model for the particles recoiling against the  $W/Z$  boson has two components, a "hard" component, that models the  $p_T$  of the  $W/Z$  boson, and a "soft" component, that models detector noise and underlying events. For the latter we use the transverse momentum imbalance  $\vec{p}_T^{mb}$  from minimum bias events recorded in the detector. The observed recoil transverse momentum is then given by

$$\vec{u}_T = -[R_{rec}(q_T) \otimes \sigma_{rec}(q_T)]\hat{q}_T - \Delta u_{\parallel}\hat{p}_T(e) + \alpha_{mb}\vec{p}_T^{mb} \quad (2)$$

where  $q_T$  is the generated value of the boson transverse momentum,  $R_{rec}$  is the response,  $\sigma_{rec}$  the resolution of the hadronic calorimeter,  $\Delta u_{\parallel}$  is the transverse energy flow into the electron window from the underlying event and pileup events,  $\hat{p}_T(e)$  is the electron direction, and  $\alpha_{mb}$  is a correction factor that allows us to adjust the resolution to the data. The hadronic momentum response is modelled with one parameter  $\kappa$ :  $R_{rec}(q_T) = \kappa \times q_T$  and the hadronic energy resolution is modelled with two parameters  $S_{HAD}$  (sampling term) and  $C_{HAD}$  (constant term):  $\sigma_{rec}(q_T)/q_T = \sqrt{C_{HAD}^2 + S_{HAD}^2/q_T}$ .

We generate  $Z \rightarrow ee$ ,  $Z/\gamma^* \rightarrow ee$  and  $W \rightarrow e\nu$  events with the PYTHIA generator and CTEQ6 parton distribution function (PDF) sets [10], then smear the generated  $\vec{p}_T(e)$  and  $\vec{u}_T$  vectors using the formulae described above and apply selection efficiencies introduced by the trigger and event selection requirements. The model parameters are adjusted to match the data.

The electron energy scale and energy offset are obtained by plotting the di-electron invariant mass of  $Z \rightarrow ee$  events and adjusting the two parameters until the Monte Carlo distribution agrees with the data; the energy scale is determined to be  $\alpha = 1.0054 \pm 0.0010$  and the energy offset is  $\beta = 0.038 \pm 0.048$  GeV.

The energy resolution for electrons is described by sampling and constant terms. In the Monte Carlo simulation, we use a sampling term of 15%  $\text{GeV}^{1/2}$  derived from Run I beam tests, and assign a 3% uncertainty to this value. We

constraint the constant term to  $C_{EM} = (4.20 \pm 0.23)\%$  by requiring that the width of the dielectron invariant mass spectrum predicted by the Monte Carlo simulation be consistent with the  $Z$  data. Figure 2 shows the invariant mass distribution for data and Monte Carlo.

The response of the detector to the underlying event relative to its response to electrons is also determined using  $Z \rightarrow ee$  events. Loosening the rapidity cuts so that one electron is required to be in the central region, while the other electron can be in central or endcap region, brings the rapidity distribution of the  $Z$  bosons closer to that of the  $W$  bosons (since there is no rapidity cut on the unobserved neutrinos in  $W$  events). In  $Z \rightarrow ee$  decays, momentum conservation requires  $\vec{p}_T^{ee} = -\vec{p}_T^{rec}$ , where  $\vec{p}_T^{ee}$  is the sum of the two electron  $p_T$  vectors. To minimize sensitivity to the electron energy resolution, we project  $\vec{p}_T^{ee}$  and  $\vec{p}_T^{rec}$  on the inner bisector of the two electron directions, called the  $\eta$  axis. Figure 3 shows the definition of the  $\eta$  axis,  $\xi$  axis is the axis orthogonal to the  $\eta$  axis. The hadronic momentum response is determined to be  $\kappa = 0.67 \pm 0.02$  by plotting  $\vec{p}_T^{ee} \cdot \hat{\eta}$  as function of  $\langle \vec{p}_T^{rec} \cdot \hat{\eta} \rangle$  and then fitting with a linear function. The sampling term for the hadronic calorimeter is determined to be  $S_{HAD} = 0.80 \pm 0.20 \text{ GeV}^{1/2}$ , and the constant term is determined to be  $C_{HAD} = 0.05 \pm 0.01$  using di-jet and  $\gamma$ +jet events.

The recoil of the  $W$  boson may affect the electron identification, especially if the recoil system is close to the electron. A measurement of the event selection biases due to the electron isolation cut can be obtained by studying the projection of the hadronic recoil momentum along the electron direction  $u_{\parallel} = \vec{p}_T^{rec} \cdot \hat{e}$ , where  $\hat{e}$  is a unit vector in the electron direction. The efficiency as a function of  $u_{\parallel}$  is fit to a function of the form:

$$\epsilon(u_{\parallel}) = \epsilon_0 \begin{cases} 1 & \text{for } u_{\parallel} < u_0; \\ 1 - s(u_{\parallel} - u_0) & \text{otherwise.} \end{cases}$$

The parameter  $\epsilon_0$  is an overall efficiency which is inconsequential for this measurement,  $u_0$  is the value of  $u_{\parallel}$  at which the efficiency starts to decrease as a function of  $u_{\parallel}$ , and  $s$  is the rate of decrease. We obtain the best fit for  $\epsilon_0 = (98.48 \pm 0.06)\%$ ,  $u_0 = -0.908 \pm 0.599 \text{ GeV}$  and  $s = 0.004364 \pm 0.000587 \text{ GeV}^{-1}$ .

The recoil  $u_T$  is corrected for the momentum that is lost by excluding the electron window. The momentum that is lost points in direction of the electron and therefore biases  $u_{\parallel}$  towards negative values. Since for  $p_T^W \ll M_W$ ,  $m_T \approx 2p_T(e) + u_{\parallel}$ , any  $u_{\parallel}$  bias directly propagates into a bias on the transverse mass. The  $u_{\parallel}$  correction ( $\Delta u_{\parallel}$ ) is very sensitive to the ratio of  $W$  events with  $u_{\parallel} > 0$  and  $u_{\parallel} < 0$ . We change the  $u_{\parallel}$  correction in the Monte Carlo simulation until it gives the same ratio as in data, giving a  $u_{\parallel}$  correction of  $-1.78 \pm 0.01 \text{ GeV}$ .

As described above, to model the detector noise and pileup, we add  $\vec{p}_T^{mb}$  from a random  $p\bar{p}$  interaction to the smeared boson  $p_T$ . Since the instantaneous luminosity profile for the recorded  $W$  and minimum bias events are different, we weight the minimum bias events so that their instantaneous luminosity approximates that of the  $W$  events.  $\alpha_{mb}$  is determined to be  $0.95 \pm 0.05$  by varying  $\alpha_{mb}$  in MC until the simulated  $u_{\parallel}$  and  $u_{\perp}$  distributions agree with the data distributions.

Finally, the distribution of the transverse momentum of  $W$  bosons  $p_T^W$  obtained in the Monte Carlo is reweighted to match the one obtained from data.

## V. BACKGROUNDS

Several processes can mimic the  $W \rightarrow e\nu$  signal: QCD events in which one jet fakes the electron and the other jet is lost in an un-instrumented region of the detector;  $Z \rightarrow ee$  decays in which one electron remains undetected and  $W \rightarrow \tau\nu \rightarrow e\nu\nu\nu$  decays.

QCD processes can fake the signature of a  $W \rightarrow e\nu$  decay if a hadronic jet fakes the electron signature and the transverse momentum balance is mismeasured. In order to subtract QCD background from  $W$  candidates we solve two linear equations using the number of  $W$  candidates with and without the track match as well as the track matching efficiency and fake probability. The number of QCD background is extracted from the following equations:  $N = N_W + N_{QCD}$  and  $N_{trk} = \epsilon_{trk}N_W + f_{QCD}N_{QCD}$ , where  $N_W$  is the true number of real  $W$  bosons, and  $N_{trk}$  and  $N$  are the numbers of  $W$  candidate events with and without track matching requirement.  $\epsilon_{trk}$  is the track matching efficiency and  $f_{QCD}$  is the track match fake probability.

$\epsilon_{trk}$  is measured from  $Z \rightarrow ee$  events by requiring a tight cut on one electron and a loose cut on the second, the loose electron is thus an unbiased sample for us to study the track matching efficiency.  $f_{QCD}$  is measured from events in which an electromagnetic cluster passing all the electron identification requirements with the exception of the track matching recoils against a jet. These events are really di-jet events where one jet has been misidentified as an EM object. To remove  $W$ +jets background from this sample, we also require  $\cancel{E}_T < 15 \text{ GeV}$ .  $f_{QCD}$  is defined as the fraction of the events in which the EM object is also found to have a matched track.

To estimate the fraction of  $Z \rightarrow ee$  events which satisfy the  $W$  selection, we use a Monte Carlo sample of 0.8 million  $Z \rightarrow ee$  events generated with PYTHIA and simulated with the full GEANT simulation.  $Z \rightarrow ee$  events typically

enter the  $W$  sample when one electron satisfies the  $W$  selection cuts while the second electron is lost or mismeasured, causing the event to have large  $\cancel{E}_T$ .

An electron is most frequently mismeasured when it goes into the ICD regions, which are covered only by the hadronic section of the calorimeter. These electrons therefore cannot be identified, and their energy is measured in the hadronic calorimeter. A large  $\cancel{p}_T$  is more likely for these events than for those in which both electrons are measured with the electromagnetic calorimeter. To select  $W$  candidates, we require that there is no second back-to-back track in azimuth with  $p_T > 15$  GeV. After this requirement the  $Z \rightarrow ee$  background in which one electron hits the ICD region or the massless gap is largely reduced. In the final data sample the  $Z \rightarrow ee$  background is found to be negligible.

The decay  $W \rightarrow \tau\nu \rightarrow e\nu\nu\nu$  is topologically indistinguishable from  $W \rightarrow e\nu$  and is suppressed by the branching fraction of  $\tau \rightarrow e\nu\nu$  and by the electron  $p_T$  cuts. The fraction of  $W \rightarrow \tau\nu \rightarrow e\nu\nu\nu$  events in the final data sample is determined using Monte Carlo to be  $(1.250 \pm 0.027)\%$ .

## VI. LIKELIHOOD FITTING

We generate a set of Monte Carlo  $M_T$  templates with  $\Gamma_W$  varying from 1.6 GeV to 3.6 GeV at intervals of 50 MeV. These templates are normalized to the number of  $W \rightarrow e\nu$  data events in the region of  $50 < M_T < 100$  GeV. The background distributions of QCD,  $Z \rightarrow ee$  and  $W \rightarrow \tau\nu$  events are added to the templates and a binned maximum likelihood is calculated for data. The fitting region is chosen to be  $100 \text{ GeV} < M_T < 200 \text{ GeV}$ . From the dependence of the likelihood on  $\Gamma_W$  (Fig. 4), we obtain the  $W$  boson width and its error as  $\Gamma_W = 2.011 \pm 0.093$  GeV. Figure 5, Fig. 6 and Fig. 7 show the data and MC comparison plots for  $M_T$ , electron  $p_T$  and missing transverse energy with the fitted  $W$  width.

## VII. SYSTEMATIC UNCERTAINTIES

The systematic uncertainties in the determination of the  $W$  width are due to effects that could alter the transverse mass distribution. Uncertainties in each input parameter of the Monte Carlo can affect the measurement of  $\Gamma_W$ . These parameters are constrained in most cases by the  $Z \rightarrow ee$  data. Since there is only a finite  $Z$  sample, there is an error associated with each part of the detector model. Although these errors are considered as systematic errors for the width measurement, they are really statistical errors which depend on the number of  $Z$  events.

To estimate the effects, we allow these input parameters to vary by one standard deviation and then re-generate the transverse mass spectrum with the same procedure used to determine the mean value of  $W$  width. If the variation of the  $W$  boson width with respect to a parameter is not linear, the error is symmetrized by assigning the larger value. A 100% uncertainty is assigned to the shift of the  $W$  width obtained when reweighting the distribution of the transverse momentum of the  $W$  boson,  $p_T^W$ .

Additional uncertainties arise from uncertainties in the value of the  $W$  mass (constrained to its world average) and from uncertainties in the production model, the parton distribution and from the effects of final state photon radiation. Pending further investigation these uncertainties are taken from our previous measurement [5].

Table I lists the uncertainties in the measured  $W$  width caused by each individual source.

## VIII. RESULTS

We have described a direct measurement of the  $W$  boson total decay width  $\Gamma_W$ , the result is  $\Gamma_W = 2.011 \pm 0.093$  (stat)  $\pm 0.107$  (syst) GeV. Figure 8 shows the  $W$  boson width results compared with the SM prediction.

## Acknowledgments

We thank the staffs at Fermilab and collaborating institutions, and acknowledge support from the Department of Energy and National Science Foundation (USA), Commissariat à L’Energie Atomique and CNRS/Institut National de Physique Nucléaire et de Physique des Particules (France), Ministry for Science and Technology and Ministry for Atomic Energy (Russia), CAPES, CNPq and FAPERJ (Brazil), Departments of Atomic Energy and Science and Education (India), Colciencias (Colombia), CONACyT (Mexico), Ministry of Education and KOSEF (Korea), CONICET and UBACyT (Argentina), The Foundation for Fundamental Research on Matter (The Netherlands), PPARC (United

| Source  | $\Delta\Gamma_W$ (MeV) |
|---|------------------------|
| EM Energy Scale                                   | 15                     |
| EM Energy Offset                                  | 17                     |
| EM Energy Resolution, Sampling                    | 30                     |
| EM Energy Resolution, Constant                    | 41                     |
| HAD Momentum Response                             | 40                     |
| HAD Energy Resolution, sampling                   | 50                     |
| HAD Energy Resolution, constant                   | 7                      |
| Primary Vertex                                    | 10                     |
| Position Resolution $\sigma_\eta$                 | 5                      |
| Position Resolution $\sigma_\phi$                 | 5                      |
| Underlying Event                                  | 47                     |
| $u_\parallel$ Correction ( $\Delta u_\parallel$ ) | 4                      |
| $u_\parallel$ Efficiency $s$                      | 1                      |
| $u_\parallel$ Efficiency $u_0$                    | 1                      |
| Selection Bias                                    | 10                     |
| QCD Backgrounds                                   | 3                      |
| $Z \rightarrow ee$ Backgrounds                    | negligible             |
| $W \rightarrow \tau\nu$ Backgrounds               | negligible             |
| $p_T^W$   | 29                     |
| $M_W$   | 15                     |
| PDF   | 27                     |
| Radiative Decays $\Delta R(e\gamma)$              | 3                      |
| Total Systematic Uncertainty                      | 107                    |
| Total Statistical Uncertainty                     | 93                     |
| Total Uncertainty                                 | 142                    |

TABLE I: Uncertainties on the  $W$  Width Measurement.

Kingdom), Ministry of Education (Czech Republic), Natural Sciences and Engineering Research Council and West-Grid Project (Canada), BMBF (Germany), A.P. Sloan Foundation, Civilian Research and Development Foundation, Research Corporation, Texas Advanced Research Program, and the Alexander von Humboldt Foundation.

- 
- [1] K. Hagiwara et. al. Phys. Rev. D66 010001 (2002).  
[2] The CDF Collaboration and the DØ Collaboration, "Combination of CDF and DØ Results on  $W$  Boson Mass and Width", hep-ex/0311039.  
[3] D. Acosta et. al. (CDF Collaboration), "First Measurements of Inclusive  $W$  and  $Z$  Cross Sections from Run II of the Tevatron Collider", hep-ex/0406078.  
[4] T. Affolder et. al. (CDF Collaboration), Phys. Rev. Lett. 85, 3347 (2000) "Direct Measurement of the  $W$  Boson Width in  $p\bar{p}$  Collisions at  $\sqrt{s}=1.8$  TeV".  
[5] V. M. Abozov et. al. (DØ Collaboration), Phys. Rev. D 66, 032008 (2002) "Direct measurement of the  $W$  boson decay width".  
[6] The LEP Collaborations ALEPH, DELPHI, L3, OPAL, the LEP electroweak Working Group, the SLD Electroweak and Heavy Flavour Groups, hep-ex/0312023.  
[7] We use a coordinated system  $(\rho, \theta, \phi)$  where  $\rho$  is the perpendicular distance from the beam line,  $\theta$  is the polar angle measured relative to the proton beam direction  $z$ , and  $\phi$  is the azimuthal angle. The pseudorapidity  $\eta$  is defined as  $-\ln(\tan\theta/2)$ .  
[8] V. Abazov, et al., in preparation for submission to Nucl. Instrum. Methods Phys. Res. A, and T. LeCompte and H.T. Diehl, "The CDF and DØ Upgrades for Run II", Ann. Rev. Nucl. Part. Sci. **50**, 71 (2000).  
[9] S. Abachi, et al., Nucl. Instrum. Methods Phys. Res. A **338**, 185 (1994).  
[10] <http://user.pa.msu.edu/wkt/cteq/cteq6pdf.html>.

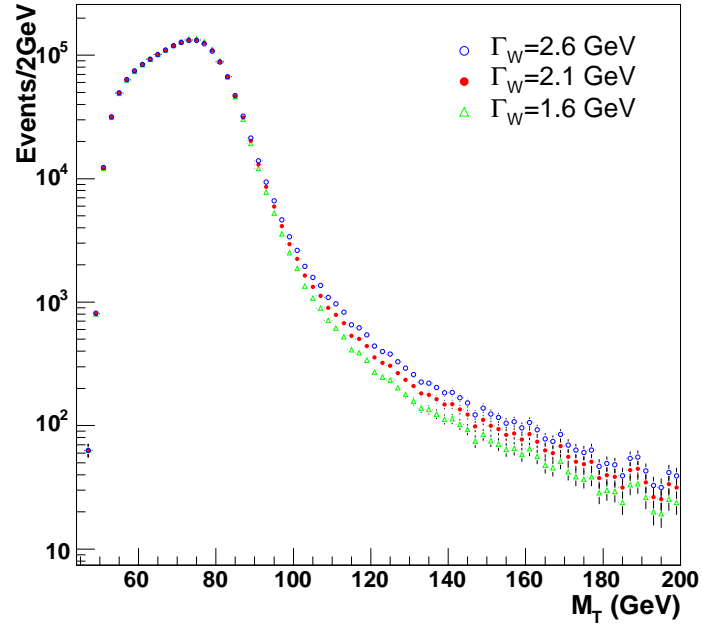


FIG. 1: Transverse mass spectra from Monte Carlo simulation with different  $W$  widths with an arbitrary normalization. The triangles are for  $\Gamma_W = 1.6$  GeV, the dots are for  $\Gamma_W = 2.1$  GeV and the circles are for  $\Gamma_W = 2.6$  GeV.

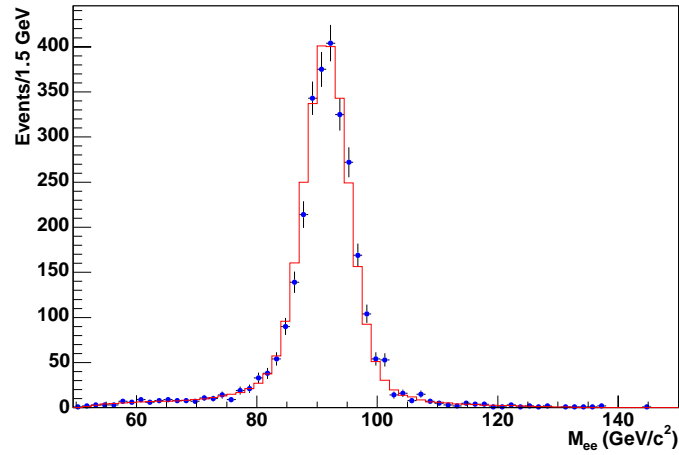


FIG. 2: Invariant Mass distribution for  $Z \rightarrow ee$  events (Blue dots for data, Red line for MC).

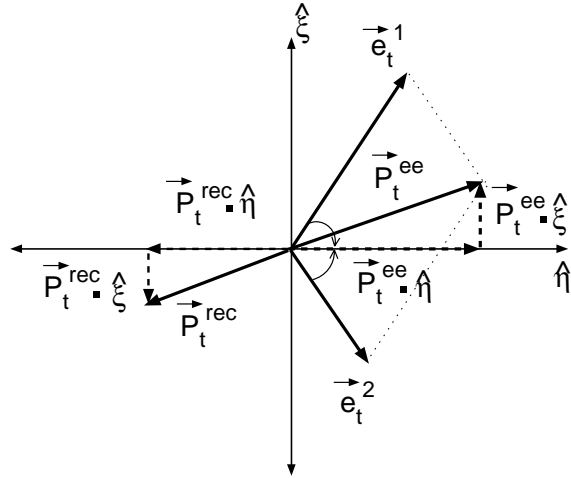


FIG. 3: Definition of  $\eta$  and  $\xi$  axis for  $Z \rightarrow ee$  events.

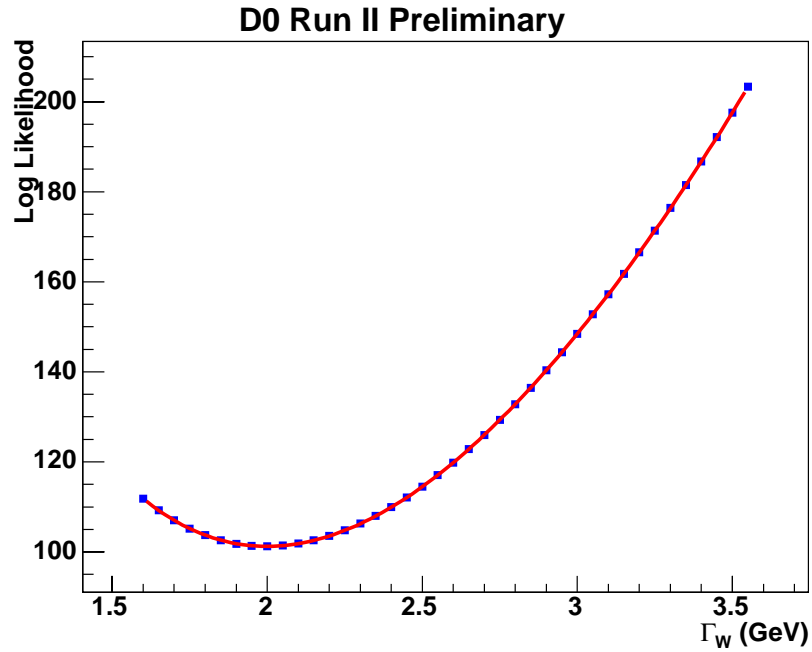


FIG. 4: Results of the maximum likelihood fit of the data to Monte Carlo templates. Monte Carlo templates are generated with  $\Gamma_W$  between 1.6 and 3.6 GeV at 50 MeV intervals. Each point represents a log-likelihood fit performed over the range  $100 < M_T < 200$  GeV. The curve is the best fit of the likelihood points to a fourth order polynomial. The best value is  $2.011 \pm 0.093$  GeV.

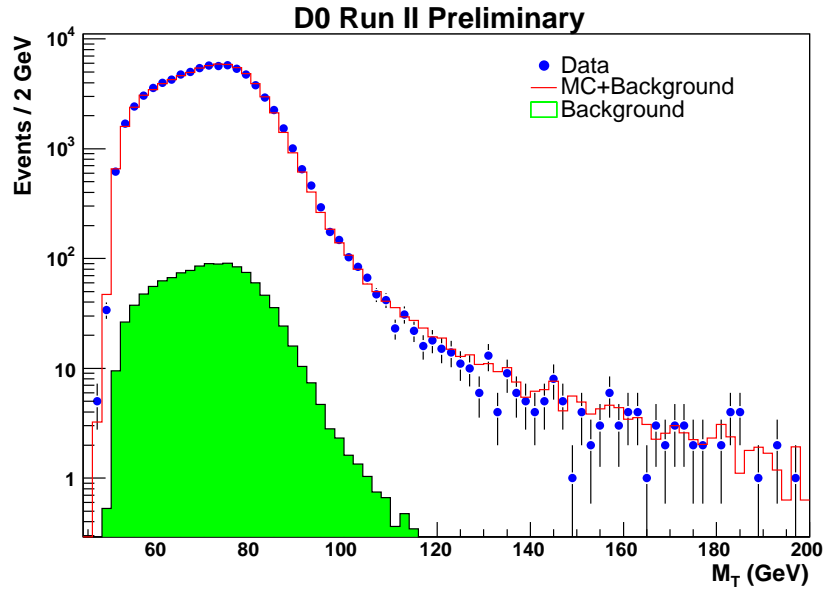


FIG. 5: Comparison of data to Monte Carlo templates for the transverse mass shape. The dots with error bars are data, the shaded area is QCD background and the line corresponds to the sum of the  $W \rightarrow e\nu$  and  $W \rightarrow \tau\nu$  Monte Carlo samples and of the QCD background for the fitted value of the  $W$  width. The normalization of the Monte Carlo samples is obtained from the transverse mass distribution in the [50, 100] GeV region, while the  $W$  width is obtained by the likelihood fit in the [100, 200] GeV region.

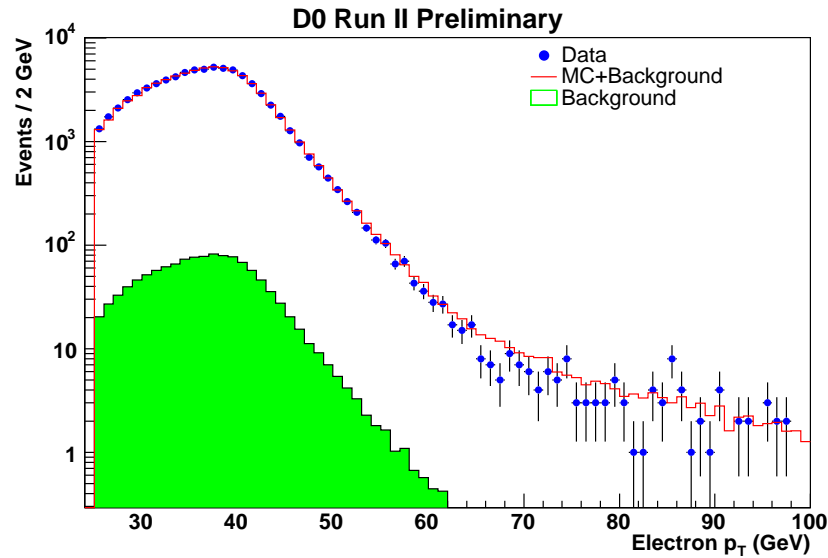


FIG. 6: Comparison of data to Monte Carlo templates for the electron  $p_T$  shape. The dots with error bars are data, the shaded area is QCD background and the line corresponds to the sum of the  $W \rightarrow e\nu$  and  $W \rightarrow \tau\nu$  Monte Carlo samples and of the QCD background for the fitted value of the  $W$  width.

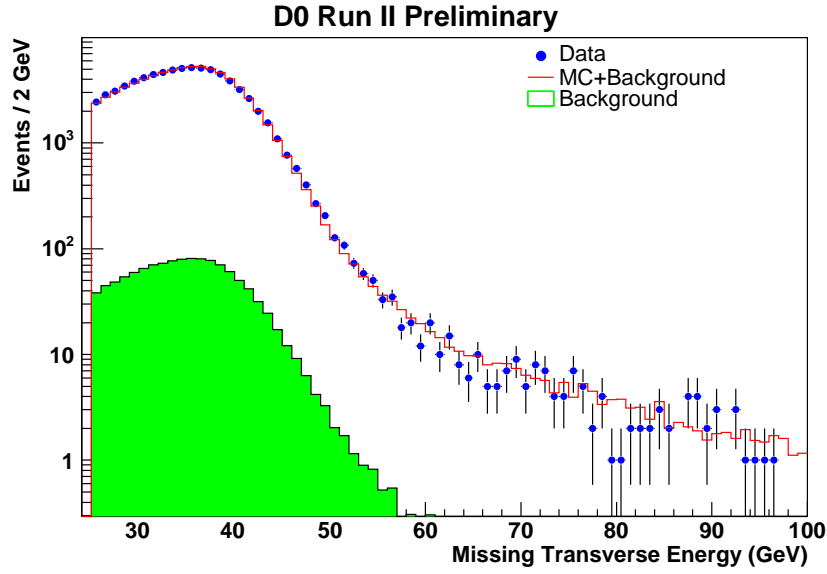


FIG. 7: Comparison of data to Monte Carlo templates for the missing transverse energy shape. The dots with error bars are data, the shadowed area is QCD background and the line corresponds to the sum of the  $W \rightarrow e\nu$  and  $W \rightarrow \tau\nu$  Monte Carlo samples and of the QCD background for the fitted value of the  $W$  width.

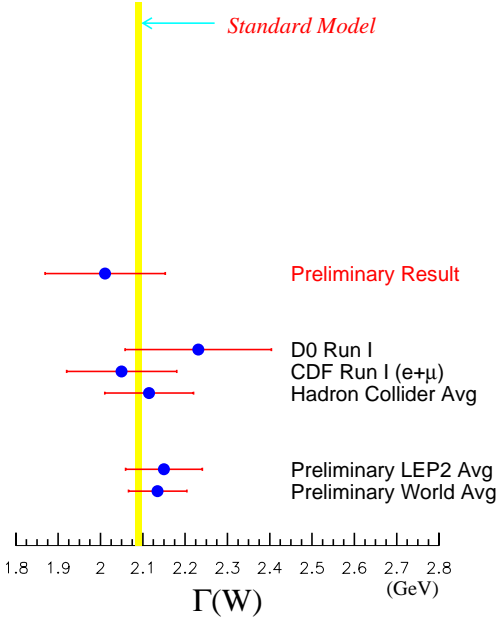


FIG. 8: Comparison of this measurement with previously published direct measurements of the  $W$  boson width. The shaded region indicates the predicted  $W$  width value.